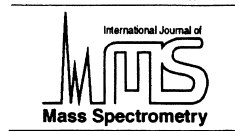




ELSEVIER

International Journal of Mass Spectrometry 203 (2000) 205–207



Subject Index

Actinides

Gas-phase californium ion chemistry, 127

Argon ions

Ab-initio-based model for the charge transfer mechanisms in $\text{Ar}^+ + \text{H}_2\text{O}$ collisions, 19

Arylalkylamines

Behaviour of arylalkylamines toward trimethyl borate as a gas-phase reagent, 101

Benzene

Kinetics of radiative/termolecular associations in the low pressure regime: reactions of bare Au^+ with benzene, 155

Binding energies

Binding energy of van der Waals- and hydrogen-bonded clusters by threshold ionization techniques, 1

Bond enthalpies

Cluster ions: Gas-phase stabilities of $\text{NO}^+ (\text{CH}_3\text{CN})_n$ and $\text{NO}_2^+ (\text{CH}_3\text{CN})_n$ with $n=1$ [en]5, 93

Borinium ions

Behaviour of arylalkylamines toward trimethyl borate as a gas-phase reagent, 101

Californium

Gas-phase californium ion chemistry, 127

Carbon dioxide

Determination of ^{16}O and ^{18}O abundance ratios in natural carbon dioxide reservoirs, 83

Carboxylic acids

Gas phase reactions of CF_3O^- and $\text{CF}_3\text{O}^-\text{H}_2\text{O}$ with nitric, formic, and acetic acid, 165

Charge transfer

Femtosecond laser mass spectroscopy of ferrocenes: Photochemical stabilization by bridged cyclopentadienyl rings?, 71

Charge-transfer reaction

Ab-initio-based model for the charge transfer mechanisms in $\text{Ar}^+ + \text{H}_2\text{O}$ collisions, 19

Chemical ionisation

Behaviour of arylalkylamines toward trimethyl borate as a gas-phase reagent, 101

Chemical ionization

Gas phase reactions of CF_3O^- and $\text{CF}_3\text{O}^-\text{H}_2\text{O}$ with nitric, formic, and acetic acid, 165

Chromium

Determination of the metastable dissociation pathways for chromium/oxygen cluster ions sputtered from potassium chromate and dichromate using the ion-neutral correlation method, 59

Cluster ions

Cluster ions: Gas-phase stabilities of $\text{NO}^+ (\text{CH}_3\text{CN})_n$ and $\text{NO}_2^+ (\text{CH}_3\text{CN})_n$ with $n=1$ [en]5, 93

Determination of the metastable dissociation pathways for chromium/oxygen cluster ions sputtered from potassium chromate and dichromate using the ion-neutral correlation method, 59

Coalescence

Significant interferences in the post source decay spectra of ion-gated fullerene and coalesced carbon cluster ions, 111

Computer modeling

Simulation-based optimization of the electrodynamic ion funnel for high sensitivity electrospray ionization mass spectrometry, 31

Delayed ionization

Significant interferences in the post source decay spectra of ion-gated fullerene and coalesced carbon cluster ions, 111

Electrospray

Simulation-based optimization of the electrodynamic ion funnel for high sensitivity electrospray ionization mass spectrometry, 31

Electrospray ionisation mass spectrometry (ESI-MS)

Analysis of oxygen-18 in orthophosphate by electrospray ionisation mass spectrometry, 177

Electrospray ionization

Charge dependence of protonated insulin decompositions, A1

Femtosecond excitation

Femtosecond laser mass spectroscopy of ferrocenes: Photochemical stabilization by bridged cyclopentadienyl rings?, 71

Ferrocenes

Femtosecond laser mass spectroscopy of ferrocenes: Photochemical stabilization by bridged cyclopentadienyl rings?, 71

Fragmentation pathways

Determination of the metastable dissociation pathways for chromium/oxygen cluster ions sputtered from potassium chromate and dichromate using the ion-neutral correlation method, 59

Fullerenes

Significant interferences in the post source decay spectra of ion-gated fullerene and coalesced carbon cluster ions, 111

Gas-phase equilibria

Cluster ions: Gas-phase stabilities of NO^+ (CH_3CN)_n and NO_2^+ (CH_3CN)_n with $n=1[en]5$, 93

Gold

Kinetics of radiative/termolecular associations in the low pressure regime: reactions of bare Au^+ with benzene, 155

Hexapole collision cell

Isotope ratio measurements of spent reactor uranium in environmental samples by using inductively coupled plasma mass spectrometry, 143

High-pressure mass spectrometer

Cluster ions: Gas-phase stabilities of NO^+ (CH_3CN)_n and NO_2^+ (CH_3CN)_n with $n=1[en]5$, 93

Hydrogen bonding

Binding energy of van der Waals- and hydrogen-bonded clusters by threshold ionization techniques, 1

Inductively coupled plasma mass spectrometry

Isotope ratio measurements of spent reactor uranium in environmental samples by using inductively coupled plasma mass spectrometry, 143

Insulin

Charge dependence of protonated insulin decompositions, A1

Intermolecular forces

Binding energy of van der Waals- and hydrogen-bonded clusters by threshold ionization techniques, 1

Ion cooling

Simulation-based optimization of the electrodynamic ion funnel for high sensitivity electrospray ionization mass spectrometry, 31

Ion/ion reaction

Charge dependence of protonated insulin decompositions, A1

Ion microprobe

Secondary ion mass spectrometry for the measurement of $^{232}\text{Th}/^{230}\text{Th}$ in volcanic rocks, 187

Ion-molecule reactions

Behaviour of arylalkylamines toward trimethyl borate as a gas-phase reagent, 101

Ion/molecule reactions

Gas phase reactions of CF_3O^- and $\text{CF}_3\text{O}^-\text{H}_2\text{O}$ with nitric, formic, and acetic acid, 165

Isotope

Analysis of oxygen-18 in orthophosphate by electrospray ionisation mass spectrometry, 177

Isotope variation measurements

Determination of ^{16}O and ^{18}O abundance ratios in natural carbon dioxide reservoirs, 83

Isotopic ratio measurements

Isotope ratio measurements of spent reactor uranium in environmental samples by using inductively coupled plasma mass spectrometry, 143

Lanthanides

Gas-phase californium ion chemistry, 127

Laser desorption

Studying noncovalent protein complexes in aqueous solution with laser desorption mass spectrometry, 49

Laser desorption/ionization

Significant interferences in the post source decay spectra of ion-gated fullerene and coalesced carbon cluster ions, 111

Laser mass spectrometry

Femtosecond laser mass spectroscopy of ferrocenes: Photochemical stabilization by bridged cyclopentadienyl rings?, 71

Ligand association

Kinetics of radiative/termolecular associations in the low pressure regime: reactions of bare Au^+ with benzene, 155

Liquid beams

Studying noncovalent protein complexes in aqueous solution with laser desorption mass spectrometry, 49

Mass analyzed threshold ionization (MATI)

Binding energy of van der Waals- and hydrogen-bonded clusters by threshold ionization techniques, 1

Mass range

Simulation-based optimization of the electrodynamic ion funnel for high sensitivity electrospray ionization mass spectrometry, 31

Mathematical modeling

Determination of ^{16}O and ^{18}O abundance ratios in natural carbon dioxide reservoirs, 83

Metal ion chemistry

Gas-phase californium ion chemistry, 127

Metaphosphate

Analysis of oxygen-18 in orthophosphate by electrospray ionisation mass spectrometry, 177

Metastable dissociation

Determination of the metastable dissociation pathways for chromium/oxygen cluster ions sputtered from potassium chromate and dichromate using the ion-neutral correlation method, 59

Multiphoton ionization

Femtosecond laser mass spectroscopy of ferrocenes: Photochemical stabilization by bridged cyclopentadienyl rings?, 71

Nitric acid

Gas phase reactions of CF_3O^- and $\text{CF}_3\text{O}^-\text{H}_2\text{O}$ with nitric, formic, and acetic acid, 165

Noncovalent interactions

Studying noncovalent protein complexes in aqueous solution with laser desorption mass spectrometry, 49

Orthophosphate

Analysis of oxygen-18 in orthophosphate by electrospray ionisation mass spectrometry, 177

Oxygen-18

Analysis of oxygen-18 in orthophosphate by electrospray ionisation mass spectrometry, 177

Oxygen isotopes

Determination of ^{16}O and ^{18}O abundance ratios in natural carbon dioxide reservoirs, 83

Plasma desorption

Determination of the metastable dissociation pathways for chromium/oxygen cluster ions sputtered from potassium chromate and dichromate using the ion-neutral correlation method, 59

Post source decay

Significant interferences in the post source decay spectra of ion-gated fullerene and coalesced carbon cluster ions, 111

Proteins

Studying noncovalent protein complexes in aqueous solution with laser desorption mass spectrometry, 49

Quadrupole ion trap

Charge dependence of protonated insulin decompositions, A1

Radiative processes

Kinetics of radiative/termolecular associations in the low pressure regime: reactions of bare Au^+ with benzene, 155

Reflectron time-of-flight mass spectrometry

Significant interferences in the post source decay spectra of ion-gated fullerene and coalesced carbon cluster ions, 111

Secondary ion mass spectrometry

Secondary ion mass spectrometry for the measurement of $^{232}\text{Th}/^{230}\text{Th}$ in volcanic rocks, 187

Simulation

Simulation-based optimization of the electrodynamic ion funnel for high sensitivity electrospray ionization mass spectrometry, 31

Space charge

Simulation-based optimization of the electrodynamic ion funnel for high sensitivity electrospray ionization mass spectrometry, 31

Spent nuclear fuel

Isotope ratio measurements of spent reactor uranium in environmental samples by using inductively coupled plasma mass spectrometry, 143

Stratospheric trace gases

Gas phase reactions of CF_3O^- and $\text{CF}_3\text{O}^-\text{H}_2\text{O}$ with nitric, formic, and acetic acid, 165

Th isotopes

Secondary ion mass spectrometry for the measurement of $^{232}\text{Th}/^{230}\text{Th}$ in volcanic rocks, 187

Trimethyl borate

Behaviour of arylalkylamines toward trimethyl borate as a gas-phase reagent, 101

Unimolecular dissociation

Charge dependence of protonated insulin decompositions, A1

Uranium

Isotope ratio measurements of spent reactor uranium in environmental samples by using inductively coupled plasma mass spectrometry, 143

U-series

Secondary ion mass spectrometry for the measurement of $^{232}\text{Th}/^{230}\text{Th}$ in volcanic rocks, 187

U-Th disequilibrium

Secondary ion mass spectrometry for the measurement of $^{232}\text{Th}/^{230}\text{Th}$ in volcanic rocks, 187

van der Waals cluster

Binding energy of van der Waals- and hydrogen-bonded clusters by threshold ionization techniques, 1

Water molecules

Ab-initio-based model for the charge transfer mechanisms in $\text{Ar}^+ + \text{H}_2\text{O}$ collisions, 19